

LIGHT NUCLIDES OBSERVED IN THE FISSION AND FRAGMENTATION OF ^{238}U

*M. V. Ricciardi⁽¹⁾, K. -H. Schmidt⁽¹⁾, J. Benlliure⁽²⁾, T. Enqvist⁽¹⁾, F. Rejmund⁽¹⁾, P. Armbruster⁽¹⁾,
F. Ameil⁽¹⁾, M. Bernas⁽³⁾, A. Boudard⁽⁴⁾, S. Czajkowski⁽⁵⁾, R. Legrain⁽⁴⁾, S. Leray⁽⁴⁾, B. Mustapha⁽³⁾,
M. Pravikoff⁽⁵⁾, C. Stephan⁽⁴⁾, L. Tassan-Got⁽³⁾, C. Volant⁽⁴⁾*

- (1) GSI – Planckstr. 1 – 64291 Darmstadt - Germany
- (2) Univ. Santiago de Compostella – E-15706 Santiago de Compostella - Spain
- (3) IPN Orsay – IN2P3, F-91406 Orsay - France
- (4) CEA Saclay – F-91191 Gif sur Yvette - France
- (5) CEN Bordeaux-Gradignan – F-33175, Gradignan - France

Abstract

Light nuclides produced in collisions of 1 A-GeV ^{238}U with protons and titanium have been fully identified with a high-resolution forward magnetic spectrometer, the fragment separator (FRS), at GSI, and for each nuclide an extremely precise determination of the velocity has been performed. The so-obtained information on the velocity shows that the very asymmetric fission of uranium, in the $^{238}\text{U} + \text{p}$ reaction, produces neutron-rich isotopes of elements down to around charge 10. New important features of the fragmentation of ^{238}U , concerning the velocity and the N/Z-ratio of these light fragments, and a peculiar even-odd structure in N=Z nuclei, have also been observed.

Introduction

In the last years, the knowledge of the formation cross sections of nuclides produced in spallation, fragmentation and fission reactions at intermediate energies has acquired an extreme importance due to the design of accelerator-driven systems and the radioactive-beam facilities. The accuracy of the predictions is determined by the description of the reaction mechanisms involved. The physics of such reactions is still a subject of research, and precise experimental data are needed to test the reliability of the theoretical estimations.

Two methods can be used to investigate the formation of nuclides in these nuclear reactions: the target fragmentation (“direct kinematics”) and the projectile fragmentation (“inverse kinematics”). The former has the advantage of employing thick targets, so also isotopes with very low formation cross sections can be produced, and the disadvantage that the identification, based on chemical techniques or on γ -spectroscopy, allows to measure only yields (mostly cumulative) of long-lived isotopes and gives no direct information on the kinematics of the reaction mechanism. In the latter, the identification of every reaction product is made on-line prior to its β -decay, and thanks to the high initial momentum of the beam, the velocity of the fragments can be measured.

Residual nuclei from ^{238}U , ^{197}Au , ^{56}Fe , ^{208}Pb beams on several targets at relativistic energies have already been produced in inverse kinematics at GSI (see F. Rejmund's contribution to this conference). In this report, we will focalize on one of the above mentioned experiments, the 1-A GeV $^{238}\text{U} + \text{H}_2$, and we will present the result of our investigation on the light residues produced in this reaction. Since the liquid H_2 target was placed inside a titanium container, it was necessary to perform a parallel experiment with a titanium dummy target of the same thickness as the windows of the titanium container. Preliminary results on both reactions (1-A GeV $^{238}\text{U} + \text{p}$ and 1-A GeV $^{238}\text{U} + \text{Ti}$) will be presented. Specifically, we will give new information concerning the light neutron-rich isotopes of elements down to around charge 10 produced in the very asymmetric fission of uranium, in the $^{238}\text{U} + \text{p}$ reaction. Also, new peculiarities of the fragmentation of ^{238}U in the interaction with titanium, such as the velocity of the light residues, the mean N/Z-ratio of the produced elements, and an enhanced production of even-even nuclei with $N=Z$, are reported.

The experiment

The experiment has been performed with a high-resolution, forward, two-stage magnetic spectrometer, the fragment separator (FRS), at GSI [1]. The primary beam of ^{238}U , at an energy of 1-A GeV, impinged on a liquid-hydrogen target, placed inside a titanium container at the entrance of the FRS. The primary-beam intensity was constantly monitored. Fragments, produced in the interaction of the beam with the target, which could cross the spectrometer, were detected at the exit of the FRS. The equipment along the FRS consisted mainly of two scintillators, placed at the intermediate image plane and at the exit, and of an ionisation chamber, placed behind the FRS (see fig. 1). The ionisation chamber recorded the energy loss of the produced ions, and from that, the nuclear charge of the reaction products was deduced. The two scintillation detectors were used to detect the horizontal positions as well as the time-of-flight between the mid-plane and the exit. The combined information on positions at mid- and final-image-plane and velocity (measured by the time-of-flight) gave a measurement of the magnetic rigidity ($B\rho$) of the ion passing through the FRS. According to the equation:

$$B\rho = \frac{A \cdot \gamma \cdot \beta \cdot c \cdot m_0}{Z \cdot e} \quad (1)$$

(where $\beta \cdot c = v$ is the velocity of the ion, γ is the relativistic parameter, m_0 the nuclear mass unit, and e the charge of an electron), the mass number A of any reaction product could be determined once the nuclear charge Z was determined. The full identification was possible for every produced nuclide, thanks to high resolutions in Z and A ($Z/\Delta Z = 150$, $A/\Delta A = 300$). Once every produced nuclide was identified (thus its mass A and charge Z were integer numbers), its velocity could easily be calculated from equation (1):

$$\gamma \cdot v = B\rho \cdot \frac{Z \cdot e}{A \cdot m_0} \quad (2)$$

with an accuracy that depends only on $B\rho$. This method gives an absolute measurement of the velocity, which does not suffer from calibration problems and produces a very accurate result. The resolution in magnetic rigidity is about $3 \cdot 10^{-4}$. In case of many events the mean value is appreciably better defined.

The full identification (A,Z) of the produced residues along with an accurate knowledge of their velocity spectra gains access to an extremely powerful and new information on the reaction in question. On the other hand the limited acceptance in magnetic rigidity of the FRS forced us to combine several $B\rho$ settings in order to cover the full range of A/Z and velocity; some lack of measurement between a setting and the next one occurred (this results in some "holes" in the data in the picture that will be presented here). Also, as a consequence of the limited angular acceptance of the FRS, only a part of the real production is detected (measurements are performed close to 0°); as we will see, this is important for the understanding of the results.

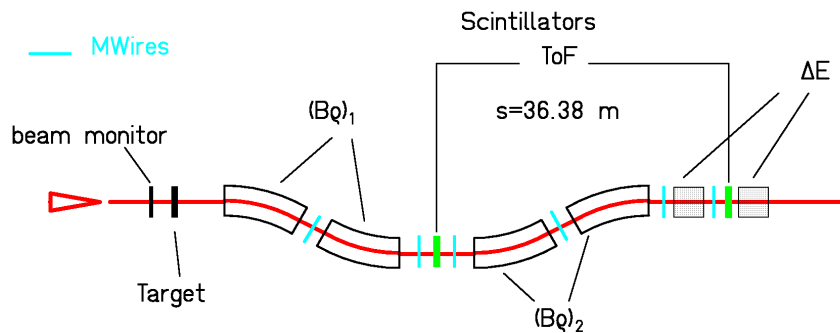


Figure 1: Schematic drawing of the fragment separator with the essential detector equipment, used in the described experiment.

A hint to the reaction mechanism

The knowledge of the spectrum of the absolute velocities for every observed isotope allows us to construct a two-dimensional cluster-plot of the velocity as a function of the element produced, as presented in fig. 2 for potassium ($Z=19$). Fig. 2-a collects the raw measured counts for the ^{238}U reactions occurring both in the H_2 target and in the windows of its titanium container; fig. 2-b refers to the interactions of ^{238}U with a titanium dummy corresponding to the walls of the container. In the abscissa the neutron number of the

produced potassium residues (i.e. every vertical line represents a potassium isotope) is reported; the ordinate gives the absolute velocity in the beam frame; the size and the colour of the clusters indicate the collected counts.

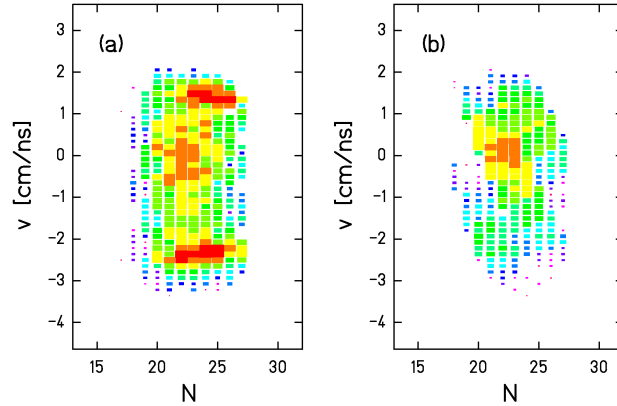


Figure 2: Two-dimensional cluster-plot of the velocity distribution as a function of the neutron number for the element potassium ($Z=19$), produced in the interaction of the uranium beam with $H_2 + Ti$ (a) and Ti alone (b). The velocity is presented in the beam frame ($v_{238U} = 0$ cm/ns).

The understanding of the velocity distributions requires a description of the reaction mechanism that leads to the formation of such nuclides. Let us consider, for instance, the velocity-spectrum for a given isotope, say ^{42}K . Projecting the line corresponding to $N=23$ on the y-axis of fig. 2-a, we observe that the velocity spectrum of ^{42}K is a triple-humped distribution with maxima around $v=1.85$ cm/ns, $v=0$ cm/ns, $v=-2.2$ cm/ns.

In fig. 3 our schematic picture of two possible processes that lead to the formation of ^{42}K is drawn. The two possible scenarios are presented in the beam frame, where the ^{238}U nucleus is at rest at the beginning. In the upper picture the ^{238}U nucleus (still) interacts with a proton, which induces an intra-nuclear-cascade inside the ^{238}U nucleus and eventually knocks out few nucleons. The excited, still very massive, pre-fragment faces now two possible competitive channels: evaporation and fission. Due to its isotropy, the evaporation process cannot change the mean value of the velocity of the pre-fragment. Things drastically change in case fission occurs. If the ^{42}K fragment is produced as a result of a binary decay, it acquires kinetic energy due to the Coulomb repulsion. Since the pre-fragments, and thus the compound nucleus, is still very massive ($210 < A < 238$, $82 < Z < 92$ according to our estimates), due to the momentum conservation, the ^{42}K fragment receives a high kinetic energy. In the second scenario, the ^{238}U nucleus interacts with the titanium nucleus through a mid-peripheral collision, which cuts a piece of the nucleus with a mechanism that is generally called "abrasion". The fissility of the so-formed pre-fragment is now very low, due to its reduced charge and mass, so fission is practically hindered and the (isotropic) evaporation of nucleons and light clusters is the only open channel. When the entire initial excitation energy is consumed to evaporate particles, the

light residual nucleus (in our case ^{42}K) has kept on average the velocity of its ancestor pre-fragment. This process is often called "fragmentation". Of course, in the case of peripheral collisions of ^{238}U with titanium, the mass of the pre-fragment is still very large, and fission is a possible channel, however the probability of producing light nuclides via fission is very low compared to that one of the fragmentation process.

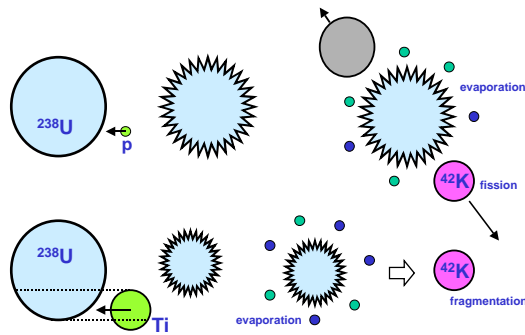


Figure 3: Schematic drawing of two possible reaction mechanisms that lead to the formation of the nuclide ^{42}K . The processes are presented in the beam (^{238}U) frame. ^{42}K can be produced both in the interaction of ^{238}U with a proton by a fission process (up) and in the interaction of ^{238}U with titanium by a fragmentation process (down).

What is actually observed at the FRS is the longitudinal component of the velocity of residues produced at about zero degrees. In figure 4-a the velocities of the ^{42}K residues produced via fission and via fragmentation are presented in the beam frame. According to our understanding of the reaction mechanism, the velocity of ^{42}K fragmentation residues fluctuates around the value of the velocity of the pre-fragment, thus its distribution is represented in the beam frame by a full, diffuse sphere. When ^{42}K is produced in a fission event, the kinetic energy that it acquires is more or less fixed, since the charge of the partner cannot be much smaller than $Z=92$, so the possible values of its velocity cover only the external shell of a large sphere. Because of the limited angular acceptance of the FRS (15 mrad around 0°), represented by a cone in the laboratory frame, only part of the real production - that one inside the cone - is actually observed. Projecting the transmitted events on the longitudinal axis, we obtain two narrow velocity distributions around points "A" and "B" and a larger one around point "C", which correspond (in the two-dimensional cluster-plot distribution) to $v \approx 1.85 \text{ cm/ns}$ and $v \approx -2.2 \text{ cm/ns}$ (humps "A" and "B") and to $v \approx 0 \text{ cm/ns}$ (hump "C"). Comparing fig. 4-b to fig. 2 we come to the conclusion that the light residues of the distributions "A" and "B" originate from fission events in the reaction $^{238}\text{U} + \text{p}$, while the light residues of the distribution "C" originate from fragmentation events in the reaction $^{238}\text{U} + \text{Ti}$.

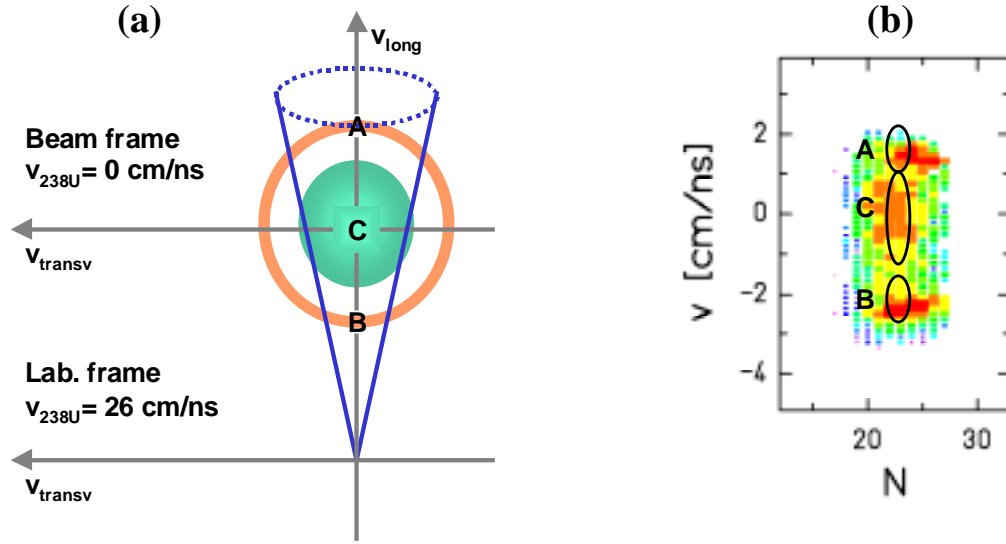


Figure 4: (a): schematic drawing of the transmitted velocities of ^{42}K , produced by fission (external shell) or via fragmentation (full sphere). The velocities are presented in the beam frame ($v_{238\text{U}} = 0$ cm/ns). The cone represents the acceptance of the FRS. The measured quantities are the projections of the velocities on the longitudinal axis, which correspond to the velocities on the ordinates of the picture on the right (b).

Results and discussion

1) Reaction: $1\text{-A GeV } ^{238}\text{U} + \text{H}_2$

1.1) Extremely asymmetric fission

In the previous section we offered an explanation of the shape of the velocity spectra of figure 2 based on the two reaction mechanisms illustrated in figure 3. Under those assumptions we concluded that the humps "A" and "B" of figure 4 are due to fission events in the interaction of ^{238}U with hydrogen. When in every two-dimensional cluster plot (like that one of figure 2-a) we squeeze all the isotopes in one line and then we combine all the lines together, we obtain figure 5. There, two circles mark the two humps "A" and "B" of the potassium isotopes. We can observe that every element shows two humps, and all the humps together form two external wings. The ridge of these wings shows a linear dependence of the velocity on the charge number Z . This linear dependence is another indication of fission [2]. Calculating the velocity from the Coulomb repulsion in the two-touching-sphere configuration at scission [3] we obtained that the velocity a fission fragment is proportional to the charge of the partner:

$$v_{\text{FRAG-1}} \approx Z_{\text{C.N.}} - Z_{\text{FRAG-1}} = Z_{\text{FRAG-2}} \quad (3)$$

Also this conditions is fulfilled by our data: in fig. 5 the velocity of a light residue is proportional to the charge of the not-observed fission fragment.

Of course, also the absolute value of the fission fragments must be consistent to the theoretical expectations. Now, according to [4] the reaction $^{238}\text{U}+p$ at 1 GeV generates a wide range of compound nuclei, from which the observed fission residues originate. Although the great part of the fission reactions occurs in nuclei with mass close to that one of uranium [4], some residues can still be generated by light compound nuclei (down to $Z=80$). As an example, the calculated theoretical [3] velocities of fission fragments originated from the compound nucleus $Z=84$, $A=214$ are presented in fig. 5 as solid lines. Analogous calculations for all the possible compound nuclei (from $Z=80$ to $Z=92$) have been performed and the corresponding lines perfectly overlap to the two fission "wings" of fig. 5. All the above considerations allow us to confirm that the counts in the two external wings are very asymmetric fission products. So in the reaction $1\text{-A GeV } ^{238}\text{U} + \text{H}_2$ heavy compound nuclei, with masses in the range between ca.180 and 238, undergo very asymmetric fission and generate extremely light fragments (at least down to $Z=10$).

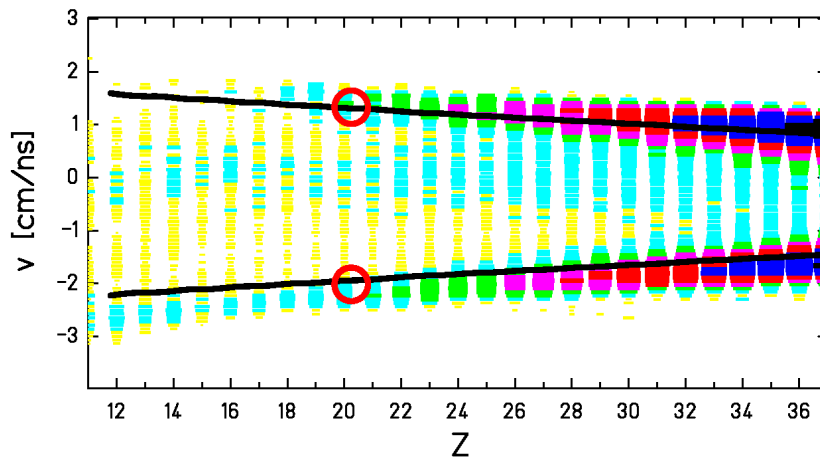


Figure 5: *Shaded area: plot of the preliminary experimental velocities versus element number. Lines: calculated velocities of fission fragments from the compound nucleus $Z=84$, $A=214$.*

Thus, very light masses (like sodium), whose formation was already observed in direct kinematics in interactions of high-energetic protons with ^{238}U [5] [6] without any information on the reaction process, are produced in very asymmetric fission events. As an example, in fig. 6 a comparison of the isotopic distributions for $Z=19$ obtained in our experiment and at ISOLDE [6] are compared. The experimental data show a high value of the A/Z -ratio of the formed isotopes; this is another sign that fission is the responsible production mechanism, since fragmentation generally produces isotopes on the neutron-deficient side of the beta-stability valley.

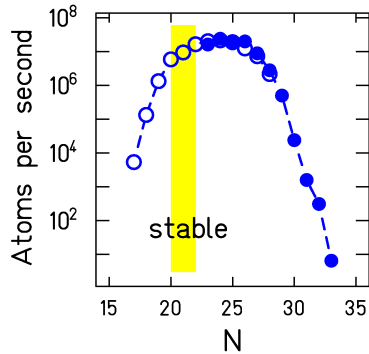


Figure 6: Potassium fission fragments from $1 \text{ A GeV } ^{238}\text{U}$ in H_2 (open dots) are compared with potassium residual isotopes from the reaction 600 MeV protons in a thick uranium carbide target (closed dots), measured at ISOLDE [6]. The counts from our experiment have been arbitrarily normalised to the ISOLDE data.

2) Reaction: $1 \text{ A GeV } ^{238}\text{U} + \text{Ti}$

2.1) Velocity of light residues

Although for many years, different measuring methods led to different descriptions of the velocity distributions of the residual nuclei, since 1989 a uniform description was offered by Morrissey [7]. Morrissey showed that the average longitudinal momentum transfer for residual nuclei with mass close to the mass of the mother nucleus ($\Delta A < 50$) increases linearly with the mass loss ΔA . Although the validity of this systematic dependence on ΔA could not be proved for large mass loss due to the uncertainties of the measurements, it seems reasonable to expect that a more violent collision, which will abrade a larger mass, will produce a larger momentum transfer.

Coming back to our experiments, in the light of what was said above, the velocity of any pre-fragment is expected to be lower than the velocity of ^{238}U , due to the momentum transfer in the reaction, and this momentum transfer is expected to grow with the mass loss ΔA . As we have already pointed out, the pre-fragment will then reach a stable configuration by an evaporation process or by fission. These processes are expected to be isotropic and will not change mean velocity of the pre-fragment. In case of fission the two fragments will run apart in opposite directions in the frame of the fissioning nucleus: the centre-of-mass velocity of the two nuclei must be equal to the velocity of the compound nucleus from which they originated, thus slightly negative. In case of fragmentation, due to the violence of the abrasion process, it is expected, according to the Morrissey's systematics, that the velocity of the pre-fragment, which will become a potassium isotope at the end of the evaporation chain, is much smaller than the velocity of the compound nucleus that will generate a potassium isotope as a fission fragment.

On the contrary, in 1993 Lindenstruth [8], analysing the residual nuclei produced in the interaction of gold with several targets, showed that for $\Delta A > 70$ the momentum transfer stops definitely to increase and eventually starts slowly to decrease. In the present experiments, the velocity of the reaction products could be determined with high precision, and this allows us to check the surprising finding of Lindenstruth.

However, we cannot compare directly the velocities of the fission and fragmentation products collected in fig.2-a. In fact, due to the limited angular acceptance of the FRS, the transmission for reaction products emitted in forward direction is slightly enhanced (see fig. 4-a). In other words, the mean value of the humps "A" and "B" of fig. 4-b does not correspond to the mean value of points "A" and "B" of fig. 4-a, by a $\Delta v = +0.03$ cm/ns; as well the mean value of the hump "C" of fig. 4-b does not correspond to the centre of the sphere in fig. 4-a, by a $\Delta v = -0.22$ cm/ns. In fig. 7-a the solid line represents the averaged mean value of the velocities of the compound nuclei from which the potassium isotopes of the humps "A" and "B" originated. Both the position of the line and the velocities of the fragmentation products of hump "C" have been corrected for the FRS transmission, under the assumption that both fission and fragmentation are isotropic processes.

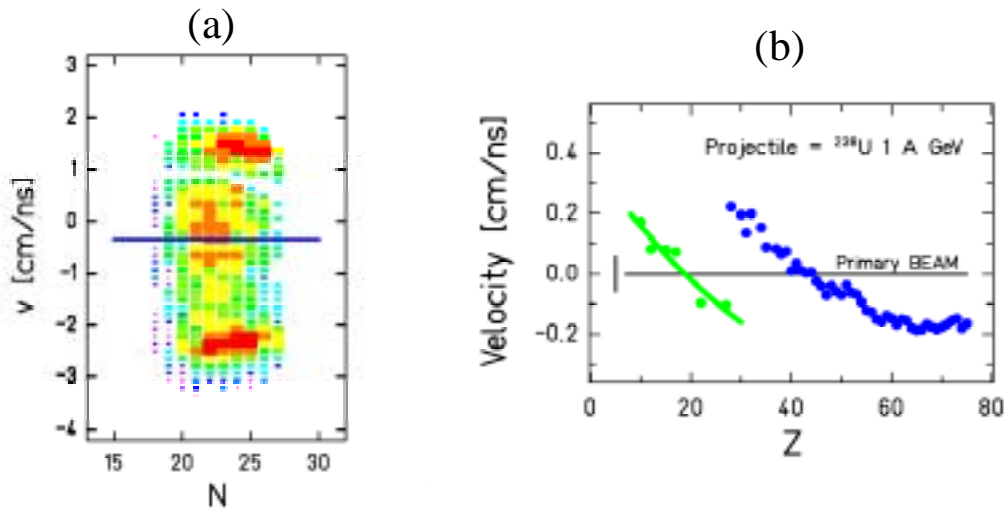


Figure 7: (a): Two-dimensional cluster-plot of the velocity distribution as a function of the neutron number for element potassium ($Z=19$), produced in the interaction of the uranium beam with $H_2 + Ti$. Data are corrected for the angular transmission of the FRS (see text). The velocity is presented in the beam frame ($v_{238U} = 0$ cm/ns). The horizontal line represents the mean velocity of the compound nuclei that generated the fission events. (b): mean velocity of the fragmentation residues produced in the reaction $1.4 \text{ GeV } ^{238}\text{U} + Ti$ (\bullet) (preliminary data) and in the reaction $1.4 \text{ GeV } ^{238}\text{U} + Pb$ [9] (\circ).

According to what previously said, the hump "C" should be much below the line of fig. 7-a. On the contrary, surprisingly enough, the potassium isotopes from fragmentation events result faster than the compound nuclei that generated the potassium fission fragments (solid line). This unrespected deceleration of the light residues can be even more clearly observed in fig. 7-b, where the mean values of the velocity-spectra of fragmentation residues are collected for several elements. Our preliminary data are compared with those obtained in the reaction $1\text{-A GeV } ^{238}\text{U} + \text{Pb}$ [9], where the acceleration of light elements is even more enhanced. Our results confirm the finding of Lindendstruth in the sense that the momentum transfer does not increase further when the mass loss becomes very important. In addition, we find an inversion of the trend for the very light products. The reason for this acceleration is not obvious. It could be connected to a possible expansion (due to compression or to thermal pressure) in the early stage of the reaction, or it could be due to the Coulomb repulsion between the surviving projectile and a charged fire streak behind it. For sure, a statistical evaporation process alone cannot provide an adequate explanation.

2.2) Mean N/Z of fragments

Let us consider again the projectile fragmentation process drawn in fig. 3. Depending on the impact parameter, the projectile will receive more or less excitation energy. Light fragments must originate in quite violent collisions (~mid peripheral), so that the pre-fragment is already appreciably lighter than the uranium projectile and it has acquired enough excitation energy to evaporate a large number of nucleons. The high excitation energy allows the pre-fragment to evaporate both neutron and proton in a competitive way, and to reduce its mass by going down along the evaporation corridor [10], which lies on the neutron-deficient side of the β -stability valley. This line, which represents the asymptotic behaviour in the statistical evaporation process, is universal and can be nicely reproduced by the semiempirical code EPAX [11]. Figure 8 reports, for every produced element, the EPAX prediction (in case of Au projectile) and the stability line [12] as a function of the mean N/Z-ratio of the isotopic distribution. These two reference lines are compared with several experimental data. Results from the reactions $800\text{-A MeV } ^{197}\text{Au} + \text{p}$ [13] and $414\text{-A MeV } ^{56}\text{Fe} + \text{p}$ [14] follow the EPAX prediction. There, the produced fragments are not far from the mother nucleus. However the reactions $1\text{-A GeV } ^{238}\text{U} + \text{Pb}$ [9], $750\text{-A MeV } ^{238}\text{U} + \text{Pb}$ [15] and $1\text{-A GeV } ^{238}\text{U} + \text{Ti}$ (this work) leave the EPAX evaporation corridor, and the more the produced light-nuclides are far from the mother nucleus, the more neutron-rich they are, up to the point that they even cross the stability line. A possible explanation could be found in the predictions of statistical multi-fragmentation models (see [16]). In these models, the light products emerge from the freeze-out of a low-density configuration. Since most of the excitation energy was spent for the disintegration of the system they are still neutron-rich and their secondary de-excitation starts from rather low temperature. Therefore these products have larger N/Z-ratios than the fragments produced as a result of evaporation from the mother nucleus.

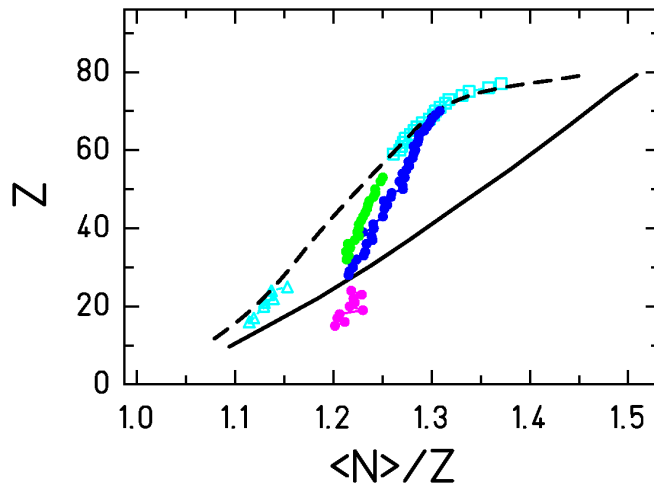


Figure 8: Mean N/Z -ratio of the isotopic distributions of the produced elements. Legend: dashed line: EPAX prediction for Au projectile [11]; solid line: stability line [12]; (\square): $800\text{-A MeV } ^{197}\text{Au} + p$ [13]; (\triangle): $414\text{-A MeV } ^{56}\text{Fe} + p$ [14]; (\bullet): $1\text{-A GeV } ^{238}\text{U} + \text{Ti}$ (preliminary data); (\bullet): $1\text{-A GeV } ^{238}\text{U} + \text{Pb}$ [9]; (\bullet): $750\text{-A MeV } ^{238}\text{U} + \text{Pb}$ [15].

2.3) Even-odd structure in $N=Z$ nuclei

Figure 9 presents the charge distribution for three different groups of produced fragments: those with the same number of protons and neutrons, $N=Z$, (left), those with $N=Z+1$ (middle) and those with $N=Z+2$ (right). In the first group of fragments ($N=Z$ fragments) a strong odd-even structure is observed, which vanishes in the second group ($N=Z+1$ fragments) and appears again, although with less intensity, in the third group ($N=Z+2$ fragments). These results are in contrast with the theoretical expectations of the statistical evaporation model, which predicts the combined effects of pairing in binding energies and level densities to cancel in such a way (the even nuclei are more bound but the level density is lower) that the formation cross sections of fragments should become approximately independent of pairing effects.

Thus, no odd-even structure should be observed. Other experimental evidences of pairing effects in the formation of nuclides have been found and reported in literature [17], [18], [19], [20]. No final information is offered for this effect, which, according to our results, seems to be connected to the internal structure of the nucleus and could be a signature for an α -clustering process. In any case these results can give us information about the structure of the nuclear level densities. Another explanation would be a deformation of the nuclear potential induced by unpaired particles. A dedicated contribution has been presented to this conference [21].

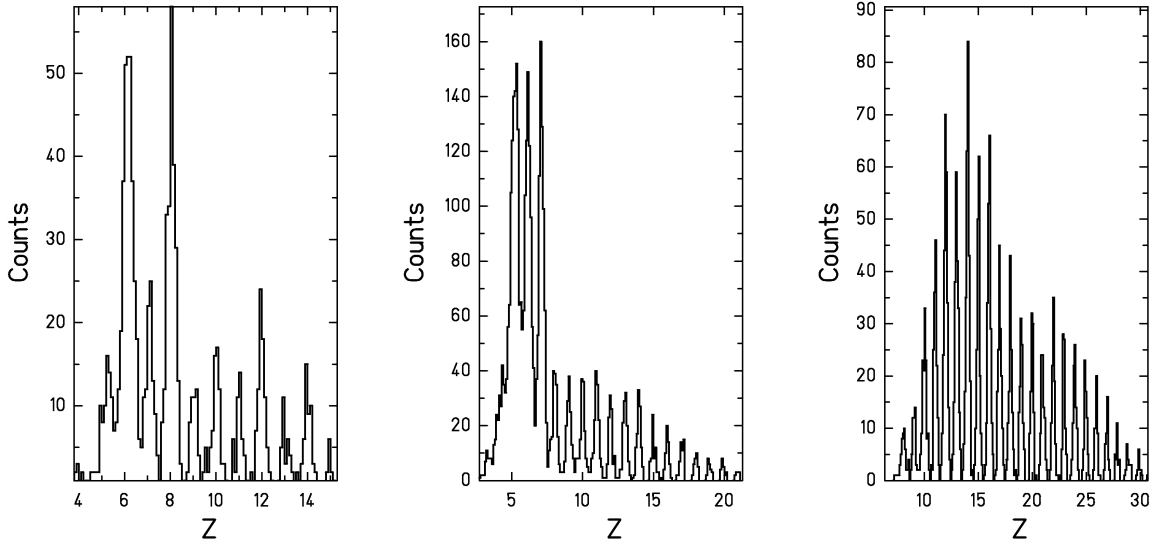


Figure 9: Charge distributions of the produced fragments with $N=Z$ (left), $N=Z+1$ (middle), $N=Z+2$ (right).

Conclusions

Light nuclides produced in collisions of 1 A· GeV ^{238}U with protons and titanium have been observed with a high-resolution forward magnetic spectrometer, the fragment separator (FRS), at GSI. All fragments were fully identified in A and Z. For each nuclide an extremely precise (resolution $\sim 10^{-4}$) determination of the velocity was performed from the Bp. The so-obtained information on the velocity gave us a new insight into the kinematics of the relativistic nuclear collisions.

Thanks to the combined results on A, Z, and the velocity of the produced fragments we discovered that the very asymmetric fission of uranium, in the $^{238}\text{U} + \text{p}$ reaction, produces neutron-rich isotopes of elements down to around charge 10. As a consequence of these results we concluded that the nuclides previously obtained at ISOLDE originated from very asymmetric fission.

Important new features of the fragmentation of ^{238}U in the interaction with Ti have also been observed. Although it is expected, due to the abrasion process, that the velocity of the surviving nucleus is reduced, these light fragments result to be accelerated. This is a possible signature of dynamic expansion in mid-peripheral relativistic heavy-ion collisions. Moreover, a detailed study of their $\langle N/Z \rangle$ showed that this ratio is greater than what is expected by the actual knowledge on the N-over-Z distribution of the fragments produced at the end of an evaporation chain in limiting fragmentation. Finally, an enhanced production of even-even nuclei with $N=Z$ was observed, which is in contrast

with the theoretical expectations of the statistical evaporation model. This could be an indication for an unexpected behavior of pairing correlation in excited nuclei or for α -clustering.

References

- 1 H. Geissel, P. Armbruster, K.-H. Behr, A. Brünle, K. Burkard, M. Chen, H. Folger, B. Franczak, H. Keller, O. Klepper, B. Langenbeck, F. Nickel, E. Pfeng, M. Pfützner, E. Roeckl, K. Rykaczewsky, I. Schall, D. Schardt, C. Scheidenberger, K.-H. Schmidt, A. Schröter, T. Schwab, K. Sümmerer, M. Weber, G. Münzenberg, T. Brohm, H.-G. Clerc, M. Fauerbach, J.-J. Gaimard, A. Grewe, E. Hanelt, B. Knödler, M. Steiner, B. Voss, J. Weckenmann, C. Ziegler, A. Magel, H. Wollnik, J.-P. Dufour, Y. Fujita, D. J. Vieira, B. Sherrill, *Nucl. Instrum. Methods* **B 70** (1992) 286
- 2 L. G. Moretto, G. J. Wozniak, *LBL-25744* (1988)
- 3 B. D. Wilkins, E. P. Steinberg, R. R. Chasman, *Phys. Rev. C* **14** (1976) 1832
- 4 B. Jurado, K.-H. Schmidt, F. Farget, T. Enqvist, F. Ameil, P. Armbruster, J. Benlliure, M. Bernas, B. Mustapha, L. Tassan-Got, C. Stephan, A. Boudard, S. Leray, R. Legrain, C. Volant, S. Czajkowski, M. Pravikoff, *Acta Phys. Polonica B* **31** (2000) 367
- 5 I. Amarel, R. Bernas, R. Foucher et al., *Phys. Lett.* **B 24** (1967) 402
- 6 H.-J. Kluge, ISOLDE user's guide, *CERN 86-05* (1986)
- 7 D. J. Morrissey, *Phys. Rev. C* **39** (1989) 460
- 8 V. Lindenstruth, *GSI-93-18* (1993)
- 9 T. Enqvist, J. Benlliure, F. Farget, K.-H. Schmidt, P. Armbruster, M. Bernas, L. Tassan-Got, A. Boudard, R. Legrain, C. Volant, C. Boeckstiegel, M. de Jong, J. P. Dufour, *Nucl. Phys.* **A 658** (1999) 47
- 10 J. P. Dufour, H. Delagrange, R. Del Moral, A. Fleury, F. Hubert, Y. Llabador, M.B. Mauhourat, K. H. Schmidt, A. Lleres, *Nucl. Phys.* **A 387** (1982) 157c
- 11 K. Sümmer, B. Blank, *Phys. Rev. C* **61** (2000) 034607
- 12 P. Marmier, E. Sheldon, "Physics of Nuclei and Particles", Academic Press (1969), pag. 36
- 13 F. Rejmund, B. Mustapha, P. Armbruster, J. Benlliure, M. Bernas, A. Boudard, J. P. Dufour, T. Enqvist, R. Legrain, S. Leray, K.-H. Schmidt, C. Stéphan, J. Taieb, L. Tassan-got, C. Volant, "Measurement of isotopic cross sections of spallation residues in 800 A MeV $^{197}\text{Au} + p$ collisions", Accepted by *Nucl. Phys.* **A** (2000)

- 14 W. R. Webber , J. C. Kish , J. M. Rockstroh , Y. Cassagnou , R. Legrain , A. Soutoul , O. Testard , C. Tull, *Astr. Jour.* **508** (1998) 949
- 15 J. Benlliure, P. Armbruster, M. Bernas, C. Boeckstiegel, S. Czajkowski, C. Donzaud, H. Geissel, A. Heinz, C. Koshuharov, Ph. Dessagne, G. Muenzenberg, M. Pfuetzner, C. Stephan, K.-H. Schmidt, K. Suemmerer, W. Schwab, L. Tassan-Got, B. Voss, *Eur. Phys. J. A* **2** (1998) 193
- 16 A. S. Botvina, I. N. Mishustin, M. Begemann-Blaich, J. Hubele, G. Imme, I. Iori, P. Kreuzt, G. J. Kunde, W. D. Kunze, V. Lindenstruth, U. Lynen, A. Moroni, W. F. J. Mueller, C. A. Ogilvie, J. Pochodzalla, G. Raciti, Th. Rubehn, H. Sann, A. Schuettauf, W. Seidel, W. Trautmann, A. Woerner, *Nucl. Phys. A* **584** (1995) 737
- 17 J.-J. Gaimard, K.-H. Schmidt, *Nucl. Phys. A* **531** (1991) 709
- 18 C. Zeitlin, L. Heilbronn, J. Miller, S. E. Rademacher, T. Borak, T. R. Carter, K. A. Frankel, W. Schimmerling, C. E. Stronach, *Phys. Rev. C* **56** (1997) 388
- 19 P. Vogel, *Nuc. Phys. A* **662** (2000) 148
- 20 C. N. Knott, S. Albergo, Z. Caccia, C.-X. Chen, S. Costa, H. J. Crawford, M. Cronqvist, J. Engelage, P. Ferrando, R. Fonte, L. Greiner, T. G. Guzik, A. Insolia, F. C. Jones, P. J. Lindstrom, J. W. Mitchell, R. Potenza, J. Romanski, G. V. Russo, A. Soutoul, O. Testard, C. E. Tull, C. Tuve´, C. J. Waddington, W. R. Webber, J. P. Wefel, *Phys. Rev. C* **53** (1996) 347
- 21 K.-H. Schmidt, contribution to this conference.